

Spectroelectrochemistry of Porphyrin Containing Mono- and Hetero-Bimetallic Systems: Porphyrin-Ru(bpy)$_3$ Conjugates

Juha M. Lintuluoto,[#] Victor V. Borovkov, Guy A. Hembury, and Yoshihisa Inoue*

Entropy Control Project, ICORP, JST, 4-6-3 Kamishinden, Toyonaka 560-0085

(Received July 22, 2002)

The redox behavior of porphyrin-Ru(bpy)$_3$ conjugates is studied by means of spectroelectrochemistry. The redox potentials for the porphyrin freebase, zinc and manganese derivatives are measured and compared to the corresponding monomeric reference porphyrins. Among the porphyrin-Ru(bpy)$_3$ conjugates, the manganese derivative behaved like its monomeric reference compound, the zinc derivative showed moderate differences, and the freebase derivative exhibited the largest differences. These results are understood to originate from the extended orbital overlap of the redox reaction centers. In the case of the freebase derivative, the bpy ligand of the Ru(bpy)$_3$ moiety is spacially very close to one of the porphyrin moiety's π-system pyrroles, which is acting as a redox reaction center. For the zinc derivative this effect is more moderate; and because the redox reactions in the manganese derivative occur at the manganese central metal, which is too far from the bpy group, the effect is minimal. From the viewpoint of the Ru(bpy)$_3$ moiety, the redox reactions of the Ru metal are not affected by the presence of the porphyrins due to the absence of Ru-porphyrin orbital overlap.

Heterometallic redox pairs are found in many systems ranging from technical applications to in vivo organisms; thus the understanding of their redox properties is essential for the further development of molecular sensors, catalysts, photovoltaic elements and potentially powerful electrochemical therapeutics. Porphyrins (por) are widely present in various electrochemical[1–3] and photochemical[4,5] as well as catalytic[6] and photocatalytic[7–9] systems, due to the unique physicochemical characteristics of their π-electron rich macrocycle, which can additionally contain a wide selection of metal ions.

The electrochemistry of Ru(bpy)$_3$ and many of its derivatives are well known and this knowledge has been used for constructing some elegant electron donor-acceptor systems based on Ru(bpy)$_3$-porphyrin conjugates.[10,11] In addition, the strong ligand centered (LC) absorption band of Ru(bpy)$_3$ at around 290 nm, which is well above the porphyrin B absorption region (390–480 nm) energy level, makes it a suitable chromophore for use in combination with porphyrins for spectroelectrochemical studies.

The advantages of using spectroelectrochemistry for studying the redox phenomena of porphyrinoids are the need for only a small amount of sample and the powerful in situ analysis of systems which have detailed and well resolved characteristic UV-vis absorption bands upon reduction/oxidation, even allowing structural information to be gained about reduced/oxidized species.

In previous work[12] we have found very efficient intramolecular fluorescence quenching of photoexcited Ru(bpy)$_3$ by manganese and iron porphyrins, which suggests that these systems may exhibit electron transfer and thus be effective redox pairs.

Tuning of the redox pair is essential for developing more effective mono and multi-metallic catalysts and molecular sensors. We present here the results of a spectroelectrochemical study of porphyrin-Ru(bpy)$_3$ conjugates **1–3** and their corresponding reference compounds **4–7** (Fig. 1), to show how, depending on the porphyrin central metal, the presence of Ru(bpy)$_3$ alters the redox potentials.

Experimental

The spectroelectrochemical measurements were done with a BAS 100B/W electrochemical workstation connected to a Shimadzu UV-3101 PC UV-VIS-NIR scanning spectrophotometer equipped with a 2 mm quartz cell, in which 80 mesh Pt was used as working electrode and AgCl as reference electrode. Dehydrated CH_2Cl_2 (Wako Chemicals) and 98+% tetrabutylammonium perchlorate (BAP) (Katayama Chemical) were used. In these conditions, the standard ferrocene oxidation Fc/Fc$^+$ potential was found to be +220 mV.

The complexes were prepared according to the previously reported methods.[12] Samples ($\sim 10^{-6}$ mol dm^{-3} of **1–3** and **5–7** and $\sim 10^{-5}$ mol dm^{-3} of **4**) were prepared by dissolving the solid substance in argon bubbled 0.1 mol dm^{-3} BAP in CH_2Cl_2. For each measurement at room temperature (293 K), the desired electrode potential was set 600 s before the scanning of the spectra (180 s). For the oxidation experiments the positive potential was increased in a stepwise manner (i.e. from 0 to +1000 mV), and for the reduction experiments the negative potential was similarly increased (i.e. from 0 to −1000 mV). Typically, the redox reactions, presented in this study, were not completely or at all reversible after experiencing large electrode potentials. The reversibility was remarkably better in the cases where only low electrode potentials were needed.

The data analyses were based on UV-vis spectral changes of the absorption bands, where isosbestic points were found, typically

Present address: Department of Chemistry, Graduate School of Science, Kyoto University, Sakyo-ku, Kyoto, 606-8502, Japan

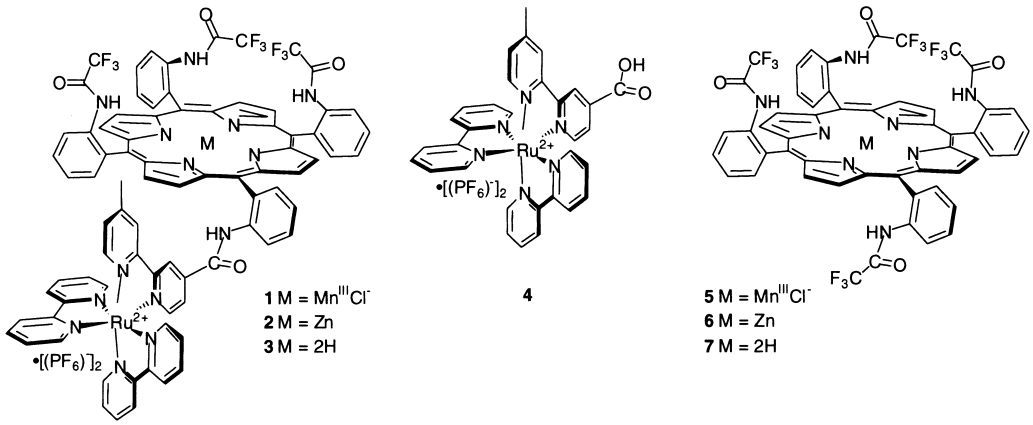

Fig. 1. Porphyrin-Ru(bpy)$_3$ conjugates **1**–**3** and their corresponding reference compounds **4**–**7** used in this study.

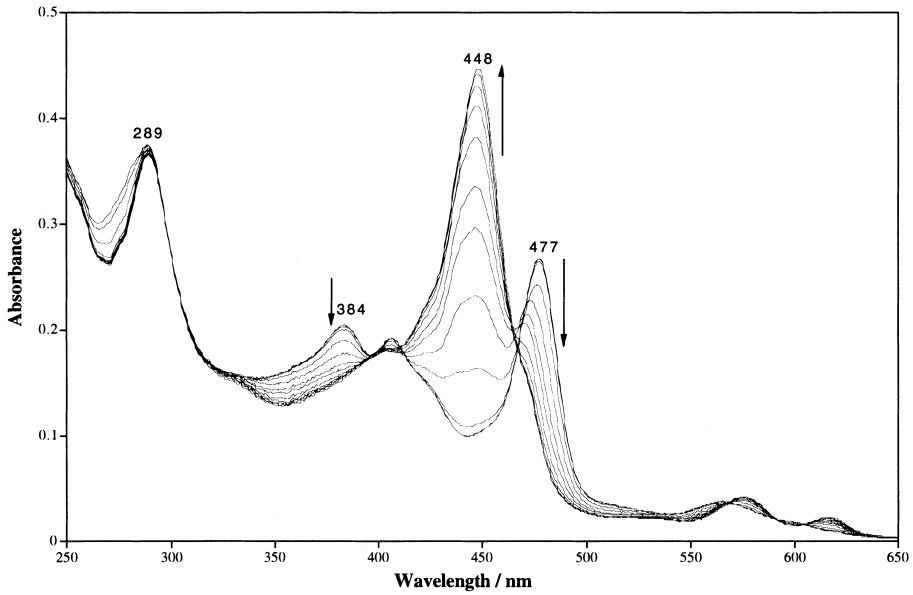

Fig. 2. Absorption spectral changes upon reduction of **1** in CH_2Cl_2/0.1 M *n*-$Bu_4N^+ClO_4^-$ at 293 K. $E_{appl.}$ = 0 mV to −550 mV.

yielding a sigmoidal curve from which the value corresponding to the mean height was taken as the formal potential (See text for an example).

Results and Discussion

Porphyrins and Ru(bpy)$_3$ possess well-resolved and intense absorption spectra which are in the red-shifted spectral region where the majority of compounds do not absorb. Porphyrins containing Mn^{III} usually have a red-shifted characteristic B (Soret) absorption band around 430–480 nm which makes them excellent UV-vis spectral probes even in the presence of other porphyrins. The absorption spectra of the manganese containing porphyrin-Ru(bpy)$_3$ conjugate (Mn(por)-Ru(bpy)$_3$) **1** clearly shows distinct major absorption bands for both components, Mn^{III}(por) (384 and 477 nm) and $[Ru(bpy)_3]^{2+}$ (289 nm) when the applied electrode potential ($E_{appl.}$) is 0 mV (Fig. 2). Upon reduction, the Mn^{III}(por) bands gradually disappear and a Mn^{II}(por) band at 448 nm appears as $E_{appl.}$ reaches −550 mV. In addition, the Q-band region (550–650 nm) experiences quantitative changes whereas the $[Ru(bpy)_3]^{2+}$ LC-band (289 nm) shows no characteristic variations for one electron reduction in this $E_{appl.}$ region. Several isosbestic points can be observed suggesting a one-step reduction process. The final spectra of the porphyrin moiety of **1** at $E_{appl.}$ −550 mV resembles very closely the spectra of Mn^{2+} tetraphenylporphyrin (Mn^{II}(tpp)) reported in the literature.[13,14]

The formal potential −390 mV for the Mn^{III}(por) → Mn^{II}(por) process was calculated independently from the 384, 448 and 479 nm bands. An example of the analysis for obtaining the formal potential is shown in Fig. 3, where the UV-vis spectral changes at 479 nm result in a sigmoidal curve from which the median absorbance is taken and its corresponding potential is set as the formal potential.

Similar reduction treatment of the compounds **4** (Ru^{2+}-(bpy)$_2$(bpyCO$_2$H) [Fig. 4(a)] and **5** (Mn^{III}(tafp)) [Fig. 4(b)], as the references for the $[Ru(bpy)_3]^{2+}$ and Mn^{III}(por) moieties of **1**, respectively, revealed the same spectral change tendencies during the change of $E_{appl.}$ from 0 to −550 mV. In this range the reference compound **5** [Fig. 4(b)] results in very similar band (384, 448 and 477 nm) behavior in comparison with **1**,

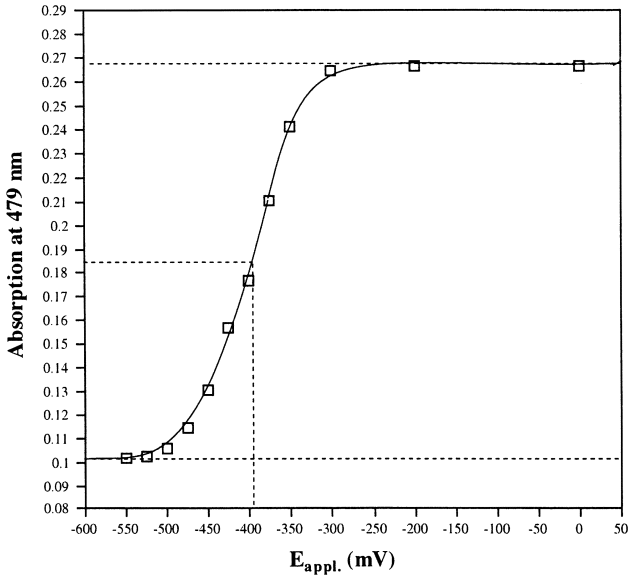

Fig. 3. The method used in this study for obtaining formal redox potentials.

with a calculated formal potential for Mn^{III}(tafp) → Mn^{II}(tafp) of −420 mV (384 nm data) also correlating with **1**. The almost invisible differences in formal reduction potentials (30 mV) in **1** and **5** suggest that the intramolecular porphyrin and $Ru(bpy)_3$ moieties in **1** are not interacting with each other when the $E_{appl.}$ is between 0 and −550 mV. Indeed, the ground state UV-vis analysis of the Q-band regions in **1** and **5** reveal no substantial differences, verifying that porphyrin and $Ru(bpy)_3$ moieties in **1** are acting independently.[15]

Reduction of **4** shows no appreciable spectral changes, and the changes attributable to the $[Ru(bpy)_3]^{2+} \rightarrow [Ru(bpy)_3]^{+}$ process which is observable when the $E_{appl.}$ is between −1200 and −2100 mV, suggest that any spectral changes of **1**–**3** at the 290 nm region in the $E_{appl.}$ range 0 to −1000 mV originate from the porphyrin moiety reduction. Spectral analysis of the LC (289 nm) or MLCT (460 nm) bands of **4** results in a formal potential of −1500 mV for $[Ru(bpy)_3]^{2+} \rightarrow [Ru(bpy)_3]^{+}$ (see Table 1), which is the same as that obtained from a cyclic voltammetric (CV) experiment.

Oxidation of **1** caused gradual disappearance of the bands of the original spectra (Fig. 5). In the case of the 289 nm band (LC of the $Ru(bpy)_3$ moiety) the diminishment correlates well with the observations upon oxidation of reference compound **4** [Fig. 6(a)], except that the disappearance is less prominent in **1**. Calculated formal potentials for the $[Ru(bpy)_3]^{2+} \rightarrow [Ru(bpy)_3]^{3+}$ oxidation in **1** and **4** were +1110 mV and +1180 mV, respectively. This result clearly shows that the oxidation in the $Ru(bpy)_3$ moiety in **1** is essentially independent of the porphyrin moiety.

The diminishment of all the characteristic bands belonging to Mn^{III}(por) moiety and the corresponding appearance of only one distinguishable new band at 665 nm suggest the formation of a $[Mn^{III}(por)]^{\bullet+}$ species in **1** (Fig. 5), where the radical cation is located in the porphyrin macrocycle rather than at the central manganese ion. These types of absorption spectra are common in the case of chlorins, where the conjugation of the otherwise identical porphyrinoid macrocycle is reduced by the presence of one C–C single bond at the meso position, instead of the double bond found in porphyrins.[16] Additionally, it has been shown that in manganese-containing porphyrins the oxidation typically occurs on the porphyrin ring in aprotic solvents.[17,18] The calculated formal potential for the formation of the $[Mn^{III}(por)]^{\bullet+}$ species in **1** was found to be +920 mV. Oxidation of the reference porphyrin **5** [Fig. 6(b)] reveals the same overall spectral changes and results in the same calculated formal potential of +920 mV, again verifying the independent na-

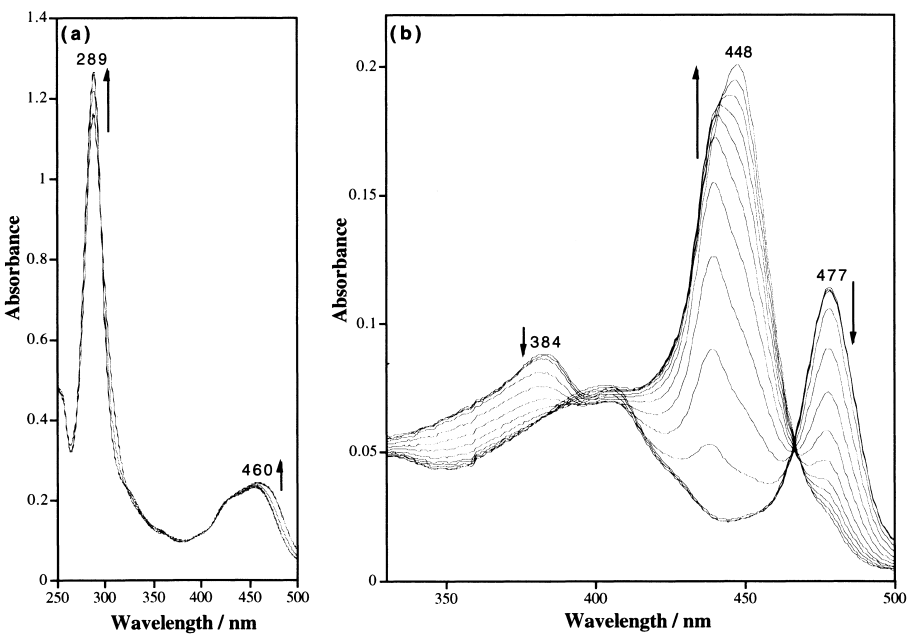

Fig. 4. Absorption spectral changes upon reduction of (a) **4** in CH_2Cl_2/0.1 M n-$Bu_4N^+ClO_4^-$ at 293 K. $E_{appl.}$ = 0 mV to −2100 mV and (b) **5** in CH_2Cl_2/0.1 M n-$Bu_4N^+ClO_4^-$ at 293 K. $E_{appl.}$ = 0 mV to −650 mV.

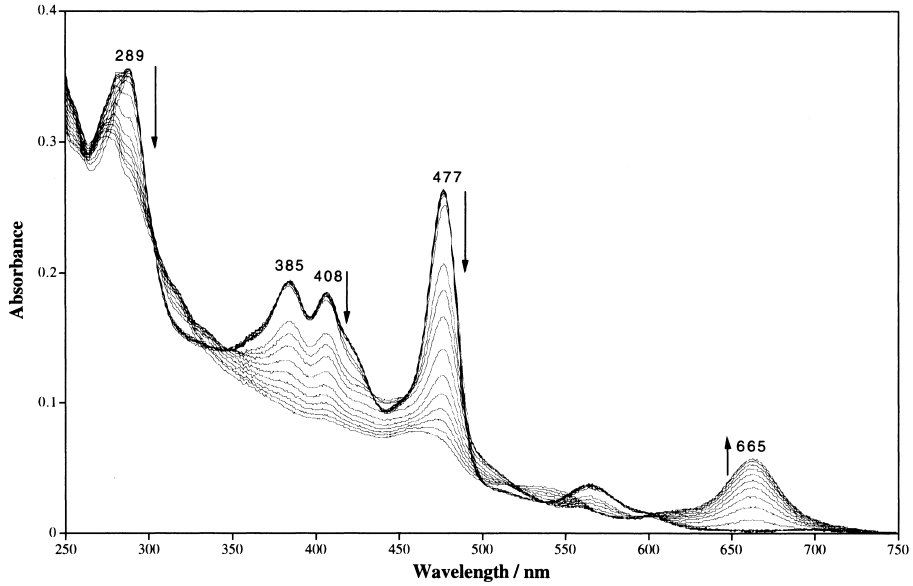

Fig. 5. Absorption spectral changes upon oxidation of **1** in CH_2Cl_2/0.1 M n-$Bu_4N^+ClO_4^-$ at 293 K. $E_{appl.}$ = 0 mV to +1500 mV.

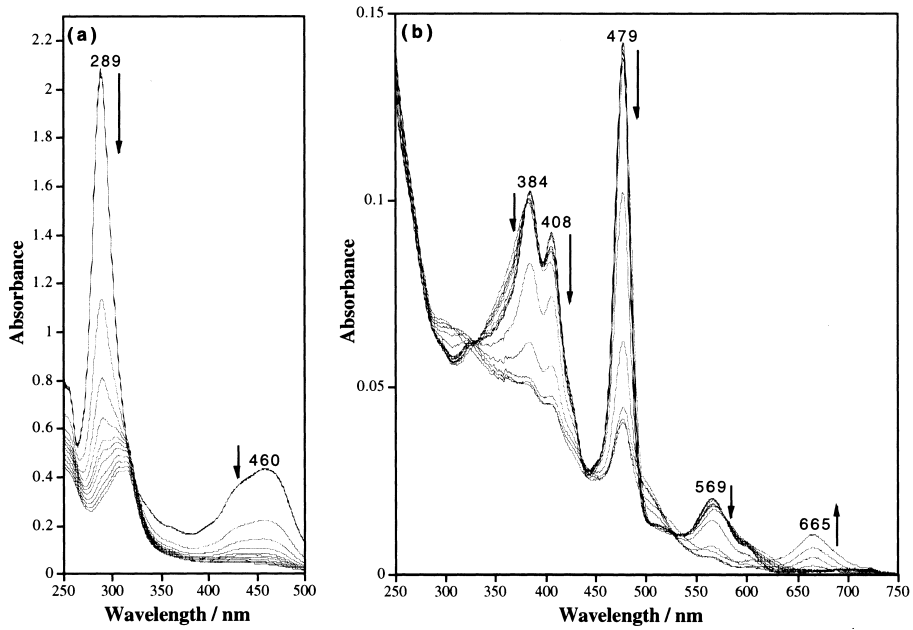

Fig. 6. Absorption spectral changes upon oxidation of (a) **4** in CH_2Cl_2/0.1 M n-$Bu_4N^+ClO_4^-$ at 293 K. $E_{appl.}$ = 0 mV to +2500 mV and (b) **5** in CH_2Cl_2/0.1 M n-$Bu_4N^+ClO_4^-$ at 293 K. $E_{appl.}$ = 0 mV to +1500 mV.

ture of the oxidation processes of the two subunits in **1**.

Reduction of the zinc containing porphyrin-Ru(bpy)$_3$ conjugate (Zn(por)-Ru(bpy)$_3$) **2** by changing the $E_{appl.}$ from 0 to −800 mV causes the disappearance of the Soret band of the Zn(por) moiety at 427 nm and the Q band at 557 nm, and results in new bands at 434 and 564 nm. This is believed to belong to the $[Zn(por)]^{\bullet-}$ species [Fig. 7(a)], as typically the radical anions of zinc porphyrins are found to appear in a more red-shifted absorption region than the neutral zinc porphyrins,[19,20] encouraging us to assign the electroreduction species as $[Zn(por)]^{\bullet-}$. The negative charge in reduced zinc containing porphyrins is believed to be located in the porphyrin core rather than at the central metal ion.[21,22] Due to the severe spectral overlap of Zn(por)-Ru(bpy)$_3$, $[Zn(por)]^{\bullet-}$-Ru(bpy)$_3$ and the second reduction product, presumably $[Zn(por)]^{2-}$-Ru(bpy)$_3$, upon changing $E_{appl.}$ from 0 to −1000 mV, quantitative analysis was difficult to perform. The formal potential for Zn(por)-Ru(bpy)$_3$ → $[Zn(por)]^{\bullet-}$-Ru(bpy)$_3$ was however estimated to be −620 mV. Reduction of the reference porphyrin **6** [Fig. 7(b)] displays spectral changes similar to those observed for **2**, but the calculated formal potentials differ notably (−950 mV for **6**). The likely reason for this is that the zinc containing porphyrin plane is highly polarized,[23] thus allowing through bond electronic interaction with peripheral Ru(bpy)$_3$ moiety. Furthermore, UV-vis spectral analysis of the Q-band regions[15] in **2** and **6** show more red-shifted absorptions (6 nm) for **2**,

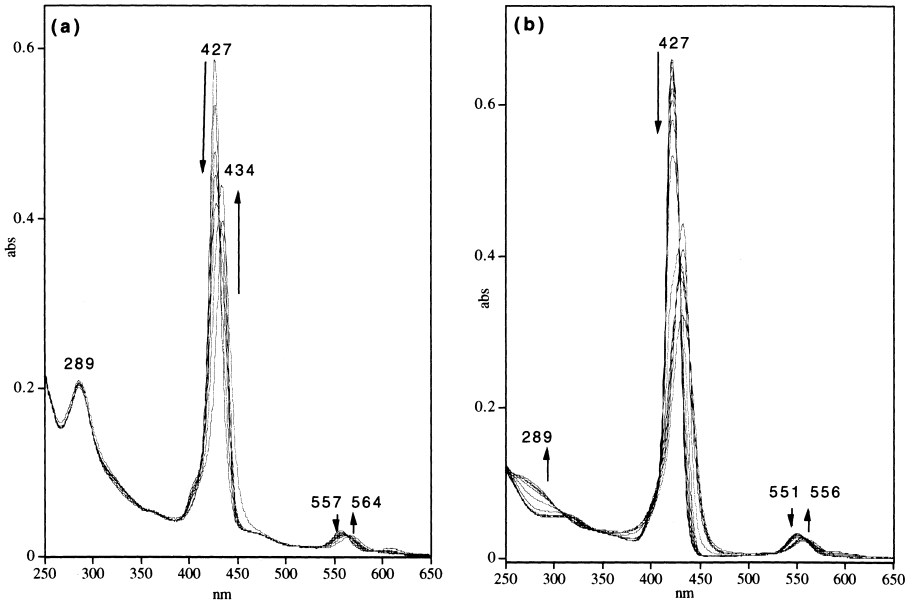

Fig. 7. Absorption spectral changes upon reduction of (a) **2** in CH_2Cl_2/0.1 M n-$Bu_4N^+ClO_4^-$ at 293 K. $E_{appl.}$ = 0 mV to −800 mV and (b) **6** in CH_2Cl_2/0.1 M n-$Bu_4N^+ClO_4^-$ at 293 K. $E_{appl.}$ = 0 mV to −1300 mV.

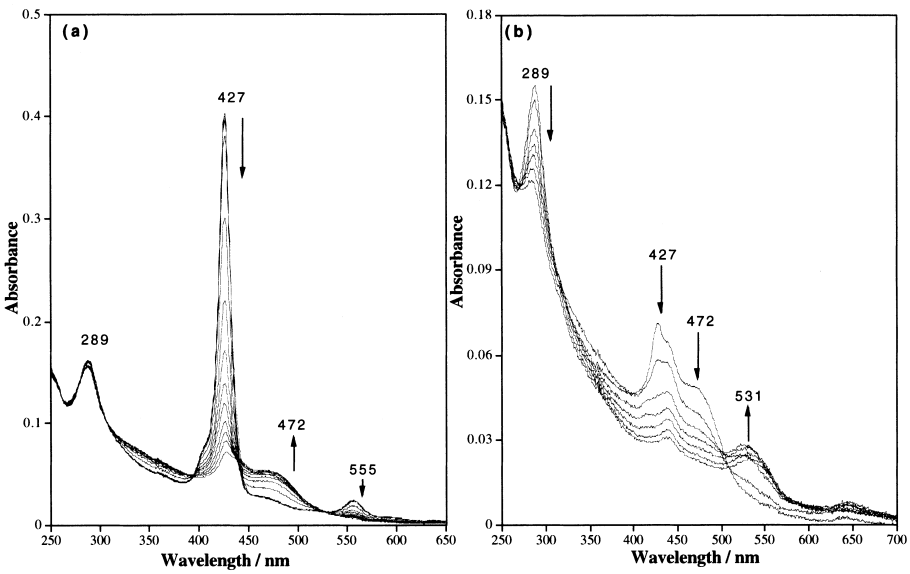

Fig. 8. Absorption spectral changes upon oxidation of (a) **2** in CH_2Cl_2/0.1 M n-$Bu_4N^+ClO_4^-$ at 293 K. $E_{appl.}$ = 0 mV to +1000 mV and (b) **2** in CH_2Cl_2/0.1 M n-$Bu_4N^+ClO_4^-$ at 293 K. $E_{appl.}$ = +1000 mV to +2000 mV.

suggesting some degree of interaction between the two subunits in **2**.

Oxidation of Zn(por)-Ru(bpy)$_3$ (**2**) causes the collapse of the Zn(por) moiety Soret band at 427 nm as well as the Q band at 555 nm [Fig. 8(a)]. The same spectral behavior was found for **6** (Fig. 9).

There is also a simultaneous formation of a new broad band at 472 nm in both **2** and **6**, but the LC band at 289 nm belonging to the $[Ru(bpy)_3]^{2+}$ moiety in **2** is found to be practically unchanged upon varying $E_{appl.}$ from 0 to +1000 mV. Oxidation of zinc containing porphyrins is known to yield a $[Zn(por)]^{\bullet+}$ species where the radical cation is delocalized around the porphyrin ring rather than at the central metal ion.[21,22] Similar spectra for other $[Zn(por)]^{\bullet+}$ species have been reported in the literature.[24–26] The calculated formal potentials for Zn(por) → $[Zn(por)]^{\bullet+}$ oxidation in **2** and **6** were +620 and +740 mV, respectively.

Varying $E_{appl.}$ from +1000 to +2000 mV leads to the disappearances of the LC band of the $[Ru(bpy)_3]^{2+}$ moiety at 289 nm as well as the band at 472 nm belonging to the $[Zn(por)]^{\bullet+}$ moiety, along with the appearance of a 531 nm band [Fig. 8(b)]. As seen in Fig. 9, the 289 nm region of the spectrum of **6** undergoes practically no changes even when $E_{appl.}$ is +1600 mV, and the observation of similar changes upon oxidation of **4** [Fig. 6(a)] jointly suggest that the changes of the 289 nm band are due to the oxidation of the Ru(bpy)$_3$ moiety in **2**. The

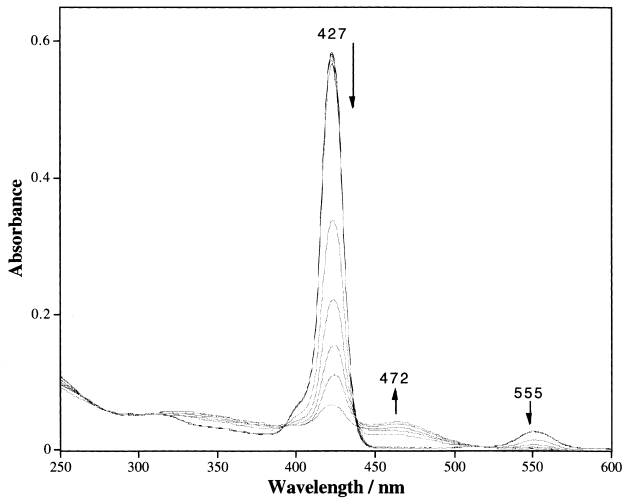

Fig. 9. Absorption spectral changes upon oxidation of **6** in CH_2Cl_2/0.1 M n-$Bu_4N^+ClO_4^-$ at 293 K. $E_{appl.}$ = 0 mV to +1600 mV.

estimated formal potential for $[Ru(bpy)_3]^{2+} \rightarrow [Ru(bpy)_3]^{3+}$ in **2** was +1180 mV, very similar to that found for the same process in **1** and **4**.

Reduction of the monometallic H_2por-$[Ru(bpy)_3]^{2+}$ (**3**) results in a new band formation at 430 nm whereas the original Soret band of the H_2por moiety at 420 nm starts to gradually disappear when the $E_{appl.}$ reaches −400 mV and finally vanishes [Fig. 10(a)]. The increase in intensity of the band at the 290 nm region of **3**, where the absorption of the $Ru(bpy)_3$ moiety also exists, starts at $E_{appl.}$ = −500 mV and stops sharply at $E_{appl.}$ = −550 mV. These changes belonging to the H_2por moiety reduction process, are also found for the H_2por moiety reference **7** [Fig. 10(b)]. The calculated formal potentials for $H_2por \rightarrow H_2por^{\bullet -}$ in **3** and **7** were −470 and −930 mV, respectively. The large potential difference indicates that the $Ru(bpy)_3$ moiety interacts strongly with freebase porphyrin π electron system and results in stabilization of the negative charge. Also, the ground state UV-vis spectral differences in the Q band region of **3** and **7** were the largest observed for any pairs in this study, resulting in a 9.5 nm blue shift of the Q_{00} band of **3** in comparison to **7**.

Upon oxidation of **3** the Soret band of the H_2por moiety at 420 nm disappears and new bands at 441 and 637 nm appear [Fig. 11(a)] this is also found for **7** under the same conditions (Fig. 12).

The LC band of the $Ru(bpy)_3$ moiety in **3** at 289 nm remains practically unchanged. Further oxidation causes the disappearance of the bands at 289, 441 and 637 nm, with the appearance of a band at 532 nm [Fig. 11(b)]. Calculated formal potentials for the $H_2por \rightarrow H_2por^{\bullet +}$ and $[Ru(bpy)_3]^{2+} \rightarrow [Ru(bpy)_3]^{3+}$ processes in **3** were +560 and +1190 mV, respectively. Comparison of the formal potentials for the $H_2por \rightarrow H_2por^{\bullet +}$ oxidation in **3** (+560 mV) and **7** (+280 mV) suggests that $Ru(bpy)_3$ moiety in **3** hinders the formation of porphyrin cation due to electronic interaction with porphyrin moiety.

Table 1 reveals that the oxidation of the $Ru(bpy)_3$ moiety in the present porphyrin-$Ru(bpy)_3$ conjugates **1**–**3** is essentially independent of the intramolecular porphyrin moiety, with the formal oxidation potential of the $Ru(bpy)_3$ moiety always much higher than that of the porphyrin moiety in **1**–**3**. These first oxidation potentials of the $Ru(bpy)_3$ moiety are considered to originate as pure $Ru^{2+} \rightarrow Ru^{3+}$ central metal oxidations, whereas the oxidation of the bpy ligands typically requires a higher energy. The porphyrin subunit does not induce conformational changes around the $Ru(bpy)_3$ structure, nor is the Ru central metal spatially close enough to the porphyrin for direct

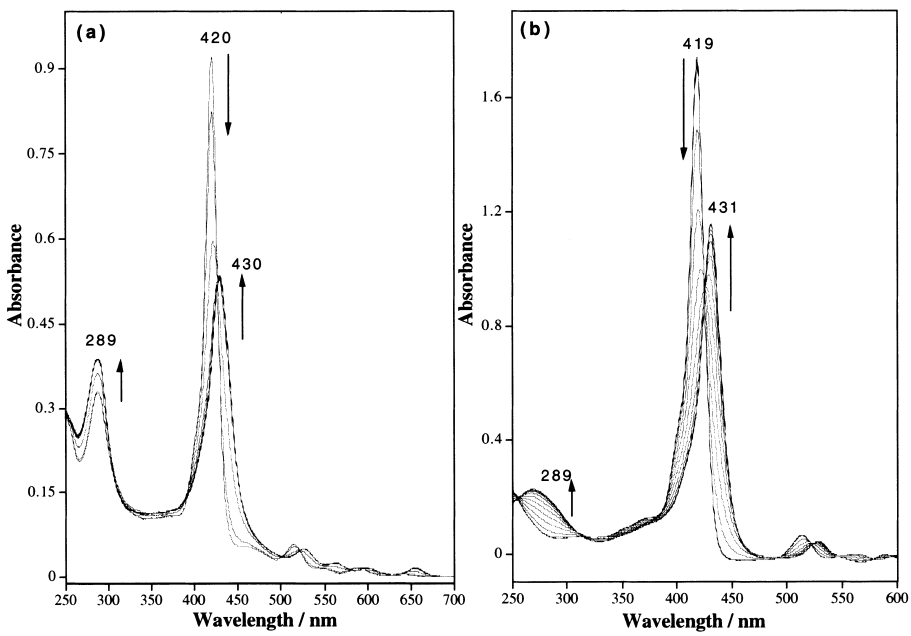

Fig. 10. Absorption spectral changes upon reduction of (a) **3** in CH_2Cl_2/0.1 M n-$Bu_4N^+ClO_4^-$ at 293 K. $E_{appl.}$ = 0 mV to −2500 mV and (b) **7** in CH_2Cl_2/0.1 M n-$Bu_4N^+ClO_4^-$ at 293 K. $E_{appl.}$ = 0 mV to −2500 mV.

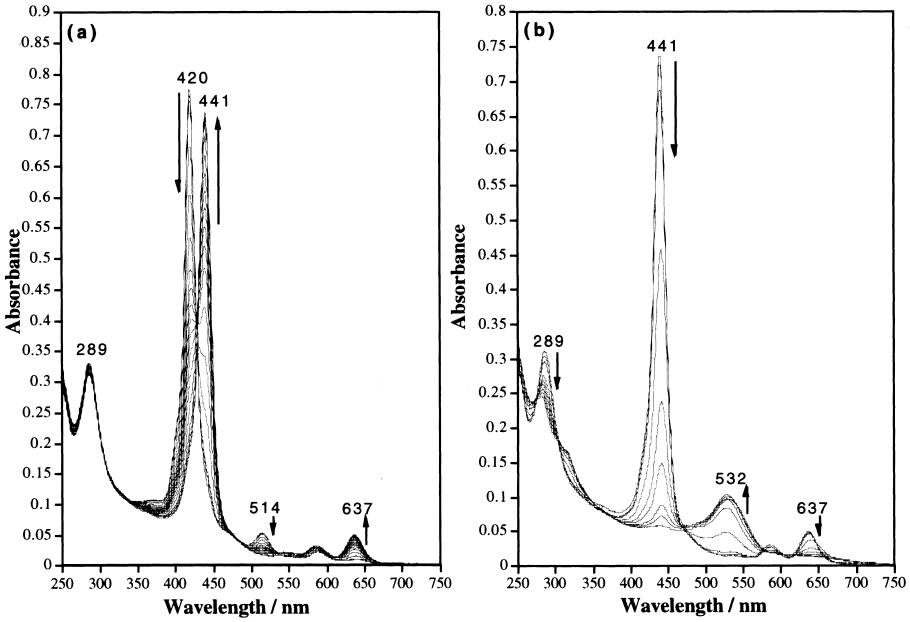

Fig. 11. Absorption spectral changes upon oxidation of (a) **3** in CH_2Cl_2/0.1 M n-$Bu_4N^+ClO_4^-$ at 293 K. $E_{appl.}$ = 0 mV to +950 mV and (b) **3** in CH_2Cl_2/0.1 M n-$Bu_4N^+ClO_4^-$ at 293 K. $E_{appl.}$ = +950 to +1500 mV.

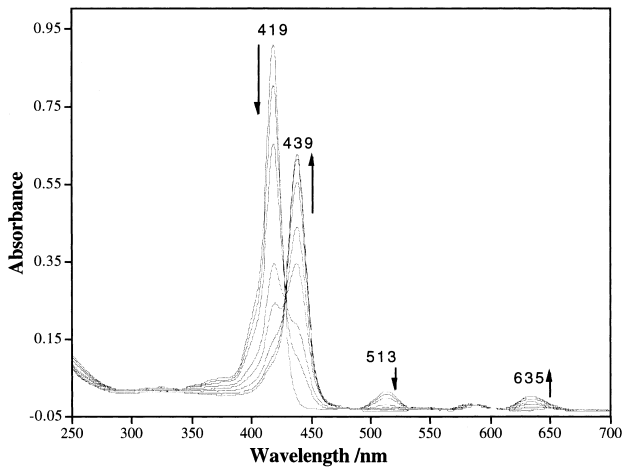

Fig. 12. Absorption spectral changes upon oxidation of **7** in CH_2Cl_2/0.1 M n-$Bu_4N^+ClO_4^-$ at 293 K. $E_{appl.}$ = 0 mV to +750 mV.

Table 1. One-Electron Oxidation and Reduction Potentials of the Porphyrin-Ru(bpy)$_3$ Conjugates **1**–**3** and Their Corresponding Reference Compounds **4**–**7** in 0.1 mol dm^{-3} Tetra-n-butyl Ammonium Perchlorate/CH_2Cl_2 at 293 K

System	Oxidation (mV)		Reduction (mV)	
	Mpor moiety	Ru(bpy)$_3$ moiety	Mpor moiety	Ru(bpy)$_3$ moiety
4	—	+1180[a)]	—	−1500[a)]
1	+920[a)]	+1110[a)]	−390[a)]	n.d.
5	+920[a)]	—	−420[a)]	—
2	+620[b)]	+1180[a)]	−620[b)]	n.d.
6	+740[b)]	—	−950[b)]	—
3	+560[b)]	+1190[a)]	−470[b)]	n.d.
7	+280[b)]	—	−930[b)]	—

a) Center metal reaction. b) Non-center metal reaction.

orbital overlap. The investigation of the ^{1}H NMR spectra of **3** and the examination of CPK molecular models of the present systems reveal that only the bpy ligands of the Ru(bpy)$_3$ moiety are spatially close to one of the pyrroles of the porphyrin moiety.

Oxidation of the porphyrin moieties can be seen to depend on both the porphyrin central metal and the Ru(bpy)$_3$ moiety. The redox properties of large variety of metalloporphyrins have been studied in depth over the past decades.[27–29] These studies showed that the reactions can occur at the central metal ion or at the porphyrin π-ring depending on the metal. Comparable results are obtained in this study for the compounds **5**, **6** and **7**. The presence of the Ru(bpy)$_3$ moiety shows an interesting effect on the tendency of the porphyrin moiety oxidation. For systems **1** and **5**, where the oxidation is considered to be a manganese central metal reaction, no effect is seen. On the other hand, the investigation of the freebase compounds **3** and **7** reveal clear differences in the first oxidation potentials, the presence of the Ru(bpy)$_3$ moiety induces a higher (ΔE = 280 mV) potential in **3** in comparison to **7**. As found by ^{1}H NMR spectroscopy, keeping in mind that the redox reactions in **3** and **7** are distributed along the porphyrin ring, one sees that the close spatial proximity which allows partial orbital overlap between the porphyrin and the bpy ligands of the Ru(bpy)$_3$ moiety is the reason for this potential difference. More support for this suggestion is seen in the case of freebase porphyrin *meso*-substituted orthogonal Ru(bpy)$_3$ complexes, in which the two subunits have hardly any orbital interaction and therefore practically no effect on the redox potentials.[30] For the zinc containing porphyrins **2** and **6** the oxidation behavior upon introduction of the Ru(bpy)$_3$ moiety yields slight decreases in potential. It is not known at present why the effect for **2** and **3** is opposite, since in both cases the oxidation of the porphyrin is sup-

posed to occur along the ring and should thus have similar orbital interactions. As mentioned earlier however, the ground-state UV-vis data suggested the strongest orbital interaction for **3** and no practical interaction for **2**. A more straightforward correlation is found when the oxidation potential differences between the porphyrin and Ru(bpy)$_3$ moieties are calculated (190, 560 and 630 mV for **1**, **2** and **3**, respectively).

The reduction of the porphyrins are found to be dependent on the central metal and the Ru(bpy)$_3$ moiety. Thus, in the presence of the Ru(bpy)$_3$ moiety the formal reduction potential of the porphyrin moiety is always lower; in manganese containing systems only slightly ($\Delta E = -30$ mV), in zinc containing systems more so ($\Delta E = -330$ mV) and in freebase systems the effect is the most dramatic ($\Delta E = -460$ mV). These results clearly support the idea of an increase in through space orbital interactions in present systems, such that the redox reaction center is directly involved in orbital overlap, and is the main reason for the differences observed in reduction potentials.

Conclusion

The change of porphyrin redox properties upon introducing the Ru(bpy)$_3$ moiety has been found to be dependent on the porphyrin central metal. In manganese containing porphyrins, the presence of the Ru(bpy)$_3$ moiety does not change the porphyrin redox properties. The reason for this may be that the redox reaction occurs solely at the manganese central metal, even if the plausible orbital overlap between one of the pyrroles of the porphyrin moiety and the bpy ligand of the Ru(bpy)$_3$ moiety exists. In the case of zinc- and freebase porphyrin-containing systems, the presence of the Ru(bpy)$_3$ moiety clearly changes the porphyrin redox behavior, apparently because the reactions occur partially/totally in the porphyrin macrocycle that interacts with the bpy ligand of the Ru(bpy)$_3$ moiety. It is also notable that the porphyrin moiety has practically no effect on the oxidation of the ruthenium in the Ru(bpy)$_3$ moiety due to the lack of orbital interaction between the ruthenium and the pyrroles of the porphyrin.

In light of these results it can be rationalized that the selection of the central metal in the porphyrinoid is important for obtaining redox potential tunability even when another redox system (such as the Ru(bpy)$_3$ moiety) is interacting at the orbital level. These observations should help to develop and choose suitable building blocks for a variety of redox applications.

References

1 I. Willner, and E. Katz, *Angew. Chem. Int. Ed.*, **39**, 1180 (2000), and references therein.

2 F.-C. Chen, S.-H. Cheng, C.-H. Yu, M.-H Liu, and Y. O. Su, *J. Electroanal. Chem.*, **474**, 52-59 (1999).

3 J. H. Cameron and S. C. Turner, *J. Chem. Soc., Dalton Trans.*, **1993**, 1941.

4 A. Maldotti, A. Molinari, R. Argazzi, R. Amadelli, P. Battioni, and D. Mansuy, *J. Mol. Cat. A: Chem.*, **114**, 141 (1996).

5 K. Araki and H. E. Toma, *J. Photochem. Photobiol. A: Chem.*, **83**, 245 (1994).

6 F. Montanari and L. Casella, "Metalloporphyrins Catalyzed Oxidations," Kluwer Academic Publishers, Dordrecht (1994).

7 A. Maldotti, A. Molinari, P. Bergamini, R. Amadelli, P. Battioni, and D. Mansuy, *J. Mol. Chem. Cat. A: Chem.*, **113**, 147 (1996).

8 A. Molinari, A. Maldotti, R. Amadelli, A. Sgobino, and V. Carassiti, *Inorg. Chim. Acta*, **272**, 197 (1998).

9 A. Molinari, R. Amadelli, V. Carassiti, and A. Maldotti, *Eur. J. Inorg. Chem.*, **2000**, 91.

10 I. Hamachi, S. Tanaka, S. Tsukiji, S. Shinkai, and S. Oishi, *Inorg. Chem.*, **37**, 4380 (1998).

11 I. Hamachi, S. Tsukiji, S. Shinkai, and S. Oishi, *J. Am. Chem. Soc.*, **121**, 5500 (1999).

12 J. M. Lintuluoto, V. V. Borovkov and Y. Inoue, *Tetrahedron Lett.*, **41**, 4781 (2000).

13 S. A. Richert, P. K. S. Tsang, and D. T. Sawyer, *Inorg. Chem.*, **27**, 1814 (1988).

14 X. H. Mu and F. A. Schultz, *Inorg. Chem.*, **43**, 3835 (1988).

15 The Q_{00}-band intensities in **1**, **5**, **2** and **6** were too small to detect in the present experimental conditions and instead the most intensive Q-bands were used for the comparisons. The use of more concentrated samples caused significant bathochromic shifts of the Q-bands in **5** and **6** apparently due to the aggregation.

16 K. M. Smith, in "Porphyrins and Metalloporphyrins Part 1," ed by K. M. Smith, Elsevier, Amsterdam (1975), pp. 3–28.

17 J.-H. Fuhrhop, K. M. Kadish, and D. G. Davis, *J. Am. Chem. Soc.*, **95**, 5140 (1973).

18 S. L. Kelly and K. M. Kadish, *Inorg. Chem.*, **21**, 3631 (1982).

19 R. A. Reed, R. Purrello, K. Prendergast, and T. G. Spiro, *J. Phys. Chem.*, **95**, 9720 (1991).

20 J. Mack and M. J. Stillman, *J. Porphyrins Phtalocyanines*, **5**, 67 (2001).

21 J.-H. Fuhrhop, in "Porphyrins and Metalloporphyrins Part 2," ed by K. M. Smith, Elsevier, Amsterdam (1975), pp. 593–662.

22 R. H. Felton, in "The Porphyrins," ed by D. Dolphin, Academic Press, New York (1978), Vol. V, pp. 53–115.

23 K. Sugiura, G. Ponomarev, S. Okubo, A. Tajiri, and Y. Sakata, *Bull. Chem. Soc. Jpn.*, **70**, 1115-1123 (1997).

24 S. Radzki, J. Mack and M. J. Stillman, *New. J. Chem.*, **16**, 583 (1992).

25 Y. Kaneko, M. Tamura and I. Yamazaki, *Biochemistry*, **19**, 5799 (1980).

26 J. Fajer, D. C Borg, A. Forman, D. Dolphin and R. H. Felton, *J. Am. Chem. Soc.*, **92**, 3451 (1970).

27 K. M. Kadish, *Prog. Inorg. Chem.*, **34**, 435 (1986).

28 A. Giraudeau, H. J. Callot, J. Jordan, I. Ezhar and M. Gross, *J. Am. Chem. Soc.*, **101**, 3857 (1979).

29 A. Wolberg and J. Manassen, *J. Am. Chem. Soc.*, **92**, 2982 (1970).

30 J. L. Sessler, V. L. Capuano and A. K. Burrell, *Inorg. Chim. Acta*, **204**, 93 (1993).